

# Surface morphology of high-temperature superconductor thin films using scanning tunnelling microscopy

M. A. HARMER, C. R. FINCHER, B. PARKINSON

*Du Pont, Central Research and Development, Experimental Station, PO Box 80328  
Wilmington, DE 19880, USA*

The surface morphology of laser-deposited superconducting  $\text{YBa}_2\text{Cu}_3\text{O}_{7-x}$  thin films has been studied using scanning tunnelling microscopy (STM). Very high resolution of the surface morphology has been obtained showing well-textured surfaces with very distinct growth patterns. The thin films produced by *in situ* laser deposition are highly oriented with typical  $J_c$  values  $> 1 \times 10^6 \text{ A cm}^{-2}$  at 77 K. The morphology of these surfaces as revealed by STM is a terraced, layer-like structure with a discrete rise of each terrace level approximately equal to the *c*-axis lattice spacing. These terraces are stacked upon each other in an ordered fashion. These terraces can also be viewed as a series of chip-like morphologies which increase in size at the lower levels. The surface structure (amount of texturing and size of terraces near the surface) shows a small but observable dependence upon the deposition conditions, with lower deposition rates producing larger grain sizes. We have also studied the chemical etching of these surfaces and the resultant morphologies have been followed using atomic force microscopy. Upon chemical etching the individual grains are revealed and due to the epitaxial growth of these films, most likely represent mutually aligned but separate grains. These etching studies provide valuable information about substructures. A model for film growth based upon nucleation and growth will be described.

## 1. Introduction

Pulsed laser ablation is very successful in growing high-quality thin films of the high-temperature superconductors (HTSC) [1, 2]. Highly oriented thin films are produced with the *c*-axis perpendicular to the substrate surface and high transition temperatures (86–91 K) and high critical currents ( $J_c$  typically  $> 1 \times 10^6 \text{ A cm}^{-2}$  at 77 K). These types of film will be useful for a number of superconducting devices ranging from electronic to microwave devices. It is clear that the growth of these films is very dependent on a number of processing conditions, for example, substrate composition, deposition rate, substrate temperature, annealing cycle, stoichiometry and final film thickness. Work has recently been directed at trying to understand processing and property correlations for these films [3–7]. This type of work is essential in order that useful and reliable devices can be developed. Surface structure, crystal orientation, degree of texture, morphology and surface roughness, will all play key roles in determining  $T_c$ ,  $J_c$ , and surface resistance, the latter being particularly important for microwave applications and overall performance of future HTSC devices.

Laser-ablated superconducting thin films have recently been studied by techniques such as transmission electron microscopy (TEM), scanning electron microscopy (SEM), X-ray diffraction and X-ray

photoelectron spectroscopy (XPS). The combined information from all of these techniques leads to an overall picture of the microstructure–property correlations of the superconductor films [5–9]. In this paper we report on the use of scanning tunnelling microscopy (STM) and atomic force microscopy (AFM) to study the growth mechanism and surface topography of thin films of  $\text{YBa}_2\text{Cu}_3\text{O}_{7-x}$  produced by *in situ* laser ablation. We observed surface microstructure which would be very difficult to observe using any of the techniques described above. The use of STM appears to be a very powerful and yet relatively simple technique for gaining detailed information on these often complex surfaces.

## 2. Experimental procedure

High-quality thin films of  $\text{YBa}_2\text{Cu}_3\text{O}_{7-x}$  were prepared by *in situ* laser deposition. The thin films were deposited by ablating a bulk superconducting target of sintered  $\text{YBa}_2\text{Cu}_3\text{O}_{7-x}$ . The ablation was carried out in a vacuum chamber ( $\sim 10^{-6}$  torr; 1 torr = 133.322 Pa) equipped with quartz windows allowing the laser beam to be incident on the sample at a  $45^\circ$  angle. The laser beam (248 nm line of a lambda Physic EMG 203 operating with KrF) was directed at the target in the chamber by a pair of plane mirrors and focused on to a  $3.0 \times 0.2 \text{ mm}^2$  spot size by

a 300 mm focal length lens placed at the entrance of the vacuum chamber. Uniform covering of the substrate was ensured by rastering the laser beam on the target with a set of motorized micrometers placed on the last plane mirror. The rastering of the laser beam inscribed a  $1\text{ cm} \times 1\text{ cm}$  square on the target, which was reconditioned to a smooth surface following each deposition. A uniform photon fluence of approximately  $1.8\text{ J cm}^{-2}$  in a 40 ns pulse was incident upon the target. For studies of the effect of deposition rate upon film surface morphology, the deposition rate was varied by the laser repetition rate. The thin films were deposited on single-crystal  $\text{SrTiO}_3$ ,  $\text{LaAlO}_3$ ,  $\text{MgO}$  or polycrystalline silver, at  $730^\circ\text{C}$  in an oxygen background pressure of 200 mtorr. Following deposition, oxygen was then bled in to the chamber and the sample allowed to cool to room temperature. The film thickness was about 100 nm unless otherwise stated.

The scanning tunnelling microscope is a Nanoscope II STM, Digital Instruments, Santa Barbara, CA. The constant current images were acquired in the  $400 \times 400$  pixel mode with scan rates from  $2.5\text{--}8.7$  lines  $\text{s}^{-1}$ . Scanning heads with ranges up to 1 and  $7\text{ }\mu\text{m}$  with the 150 V applied to the tubular piezo-elements were used. Experiments were performed using electrochemically etched platinum or tungsten tips at room temperature and in air, as described previously [10]. In all experiments, a constant tunnelling current was used between the tip and the surface. In this mode the tip moves up and down in response to the surface topography. The tunnelling voltage varied between  $+2.5$  and  $-2.5$  V sample bias; however, most of the experiments were performed with a tunnelling voltage and current of 1.0 V and 0.2 nA, respectively.

To gain further insight into the growth morphology of the thin films, the superconducting films were chemically etched using a bromine-in-methanol solution for varying lengths of time, as described in the literature [11]. Films were placed in a 0.5% bromine/methanol solution and sonicated for periods up to 5 min. The films were then sonicated in methanol for a further 5 min. In the case of the longer etching times a considerable proportion of the film was removed all the way down to the substrate. These now discontinuous, non-conducting films could not be observed by STM which requires a conducting surface. The morphology of these chemically etched surfaces was, however, studied by atomic force microscopy (AFM) which can be used on insulating as well as conducting surfaces [12].

The AFM instrumentation, like the STM, was acquired from Digital Instruments. The AFM experiments were performed in a constant force mode, rastering in the same manner as described for the STM experiments. In this case, however, the micro-machined silicon cantilever and tip is in contact with the surface and moves up and down to maintain the same force on the surface. In force microscopy the property sensed is the interaction force between the tip and sample and this interaction is translated in to a height mode by the use of the tip and cantilever. A detailed account on the use of force microscopy and STM can be found in the literature [12, 13].

### 3. Results and discussion

High-quality thin films of  $\text{YBa}_2\text{Cu}_3\text{O}_{7-x}$  have been deposited on a number of different substrates. Fig. 1 shows the X-ray diffraction pattern of a thin film showing high texture which was deposited on single-crystal  $\text{MgO}$ . The film thickness is 100 nm. The X-ray diffraction pattern shows only (001) reflections, consistent with the  $c$ -axis alignment perpendicular to the substrate and the  $a$ - $b$  plane parallel to the substrate. No additional phases are observed. Highly oriented, epitaxial grown films of  $\text{YBa}_2\text{Cu}_3\text{O}_{7-x}$  have also been deposited on the single-crystal substrates  $\text{LaAlO}_3$  and  $\text{SrTiO}_3$ . Epitaxially grown films of this kind have been described in the literature by several groups [1-4]. For example, films grown on  $\text{MgO}$ , with a lattice mismatch with the superconductor of 8.5%, have a polycrystalline structure; however, the oriented grains have mainly zero degree grain-boundary angles ( $>80\%$ ) with the remaining grain boundaries being low-angle. In the case of  $\text{SrTiO}_3$ , which has a smaller lattice mismatch ( $\sim 2.5\%$ ), the films appear essentially free from macroscopic grain boundaries or, more precisely, due to the close lattice match, the zero-angle grain boundaries cannot be observed. The coupling between such highly aligned films is very high, thus accounting for the high  $J_c$  values observed. In this study the superconducting properties of the films were all similar with  $T_c$  around 88-90 K with a narrow transition width ( $<1$  K) and high critical currents of the order of  $>1 \times 10^6\text{ A cm}^{-2}$  at 77 K.

The as-deposited films had a mirror-like finish and investigation with SEM showed these films to be both dense, smooth and relatively featureless. In some experiments, where high deposition rates were used, a small number of spherical particulates were found on the surface, in addition to a small amount of more needle-like or rectangular structures. These types of structure are well documented in the literature and have been shown to be due to a small amount non- $c$ -axis aligned  $\text{YBa}_2\text{Cu}_3\text{O}_{7-x}$  growing perpendicular to the substrate [2, 6]. Most of the surface was featureless in the SEM. When the surface morphology of these thin films was studied using STM a number of interesting features were revealed due to the STM's

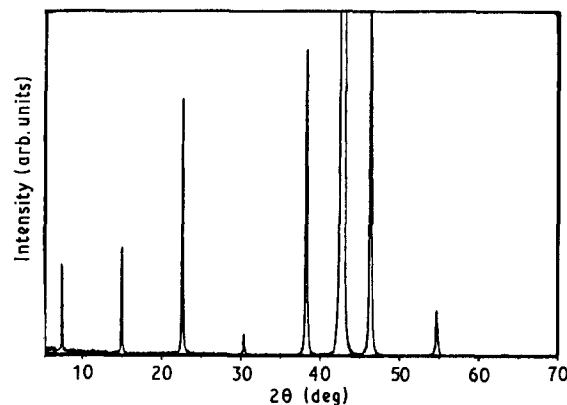


Figure 1 XRD image of a laser-deposited thin film of  $\text{YBa}_2\text{Cu}_3\text{O}_{7-x}$  on  $\text{MgO}$ , showing only 001 reflections with  $c$ -axis perpendicular alignment.

unique ability to scan  $x$ - $y$  directions of several micrometres with sub-nanometre resolution in the  $z$  direction.

Fig. 2a, shows the surface morphology of a 100 nm thick film of  $\text{YBa}_2\text{Cu}_3\text{O}_{7-x}$  on MgO. The surface appears as a network of terraces consisting of disc-like structures which will be simply described as chips. The chips appear in some cases to be stacked upon one another with the size of the chips increasing at the lower levels. This can be seen clearly in Fig. 2b showing the surface morphology of a film but at higher magnification. These stacks also form pinnacle-type structures which extend to the surface. The individual chips are reasonably smooth with the chips on the top surface being typically 10–30 nm wide while about three levels below they are more like 100–200 nm in width. The distance in the  $z$ -direction, between the various levels appears to be related to the  $c$ -axis unit cell of  $\text{YBa}_2\text{Cu}_3\text{O}_{7-x}$  with many step heights being close to 1.2 nm or multiples of 1.2 nm. The top

10–15 nm of the surface appears discontinuous. At lower levels as the chip size increases the film becomes more continuous. These chips or islands appear to coalesce at the lower levels.

Although not clearly defined, in some areas of the film the terraces come to the surface with a structure which could be consistent with other observations of spiral growth [8, 9]. Fig. 2c and d represent higher magnification images of Fig. 2a and b. The spiral-type morphology has been recently reported for sputtered films [8, 9] where the surface consists exclusively of these type of spiral networks. In our study of laser-ablated films we only saw a few of these, somewhat different from that observed for sputtered films. In the case of sputtered films, it has been proposed that the films nucleate as islands and grow by adding material to the edge of a spirally rising step, giving rise to columnar grains [9].

We have recently reported that the tip of the STM can be used to etch away material from the surface of

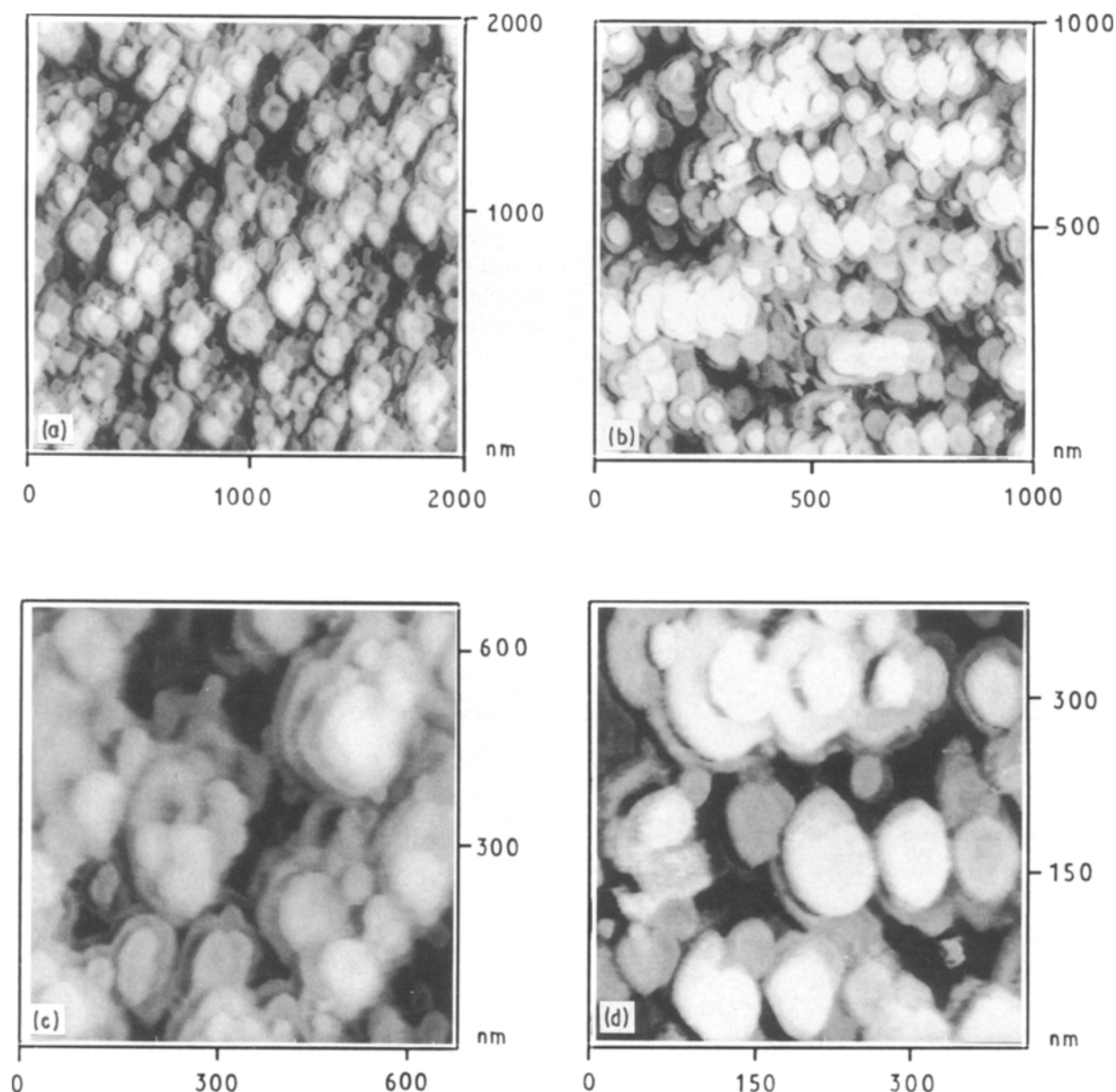


Figure 2 STM image of the surface morphology of a thin film of  $\text{YBa}_2\text{Cu}_3\text{O}_{7-x}$  on MgO, maximum distance in the  $z$ -direction is 20 nm. (a, b) Images of two different films at different magnifications. (c, d) Enlargements of (a) and (b), respectively.

superconductors [14]. Repeated rastering of the STM tip over the surface of the film for about 30 min removes numerous terrace levels near the surface. Apart from the nanofabrication aspects implied from this work [11] this method allows examination of the morphology beneath the surface. As the chips, and in some areas small islands, are removed, the substructure beneath is revealed to be more continuous (necessary to account for the high values of critical current observed in these films). Fig. 3, shows a  $\text{YBa}_2\text{Cu}_3\text{O}_{7-x}$  thin film where some of the top surface has been removed via STM etching to reveal the more continuous levels. Some chip-like islands are also still apparent.

The general morphology described, terraced hillocks, has been found on films deposited on several

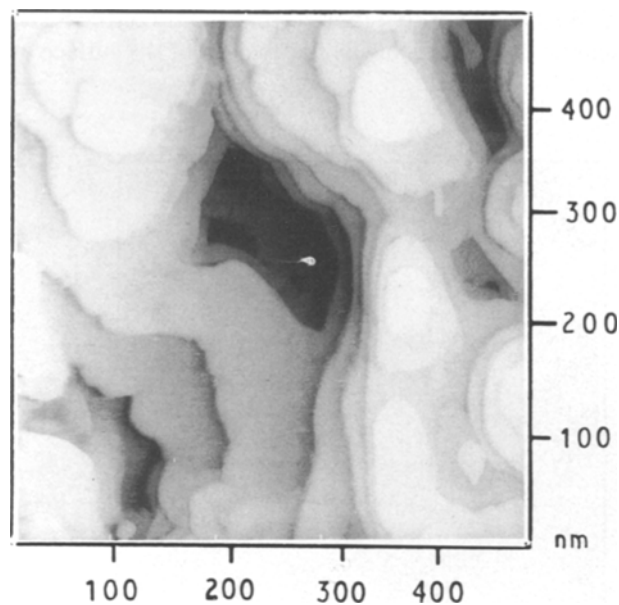


Figure 3 STM image of the surface of a thin film which has been etched by repeated rastering with the STM tip, to reveal a more continuous substructure. Note the islands and continuity at lower levels. Step heights are close to 1.2 nm or multiples of 1.2 nm.

substrates,  $\text{MgO}$ ,  $\text{SrTiO}_3$  and  $\text{LaAlO}_3$ . The surface morphology appears, in each case, to be similar. In some cases the films appear as pinnacles, where the chips and stack-like features are present, although sometimes less well-defined. The surface roughness of the films are of the order of 10–20 nm, representing the highest and lowest points measured over an area of several micrometres (up to 7000 nm). Although high-definition images have been obtained several weeks after film preparation, high definition is often greatly enhanced by use of freshly prepared STM tips and films.

The surface morphology and film characteristics have also been studied as a function of deposition rate and film thickness. The films were deposited with deposition rates varied by a factor of 50 through variation of the laser pulse frequency (1–50 Hz). Most of the experiments described in this study used a pulse rate of 25 Hz. It appears that altering the deposition rate has only a small effect on the superconducting properties, for example  $T_c$  remained at 88 K and the critical current (for the highest deposition rate film) was only slightly reduced from  $1 \times 10^6 \text{ A cm}^{-2}$  at 77 K. The negligible effect of altering the deposition rate on the superconducting properties has also been previously noted where there is no fundamental change in microstructure except for outgrowth formation [2]. Fig. 4 shows the STM images of films grown at different deposition rates. The data seem consistent with the critical current data. We see only small morphological changes as the deposition rate is varied. In particular, at the lowest deposition rate, the morphology appears to be more textured and the crystallites or chips on the top surface appear larger. The appearance of columnar structures, culminating in pinnacles are apparent in both films. Surface morphologies of films of differing thicknesses were also studied. The film thickness was varied from 10–100 nm with no discernible differences in the STM images where the usual formation of chip-like morphologies and stacked regions was observed.

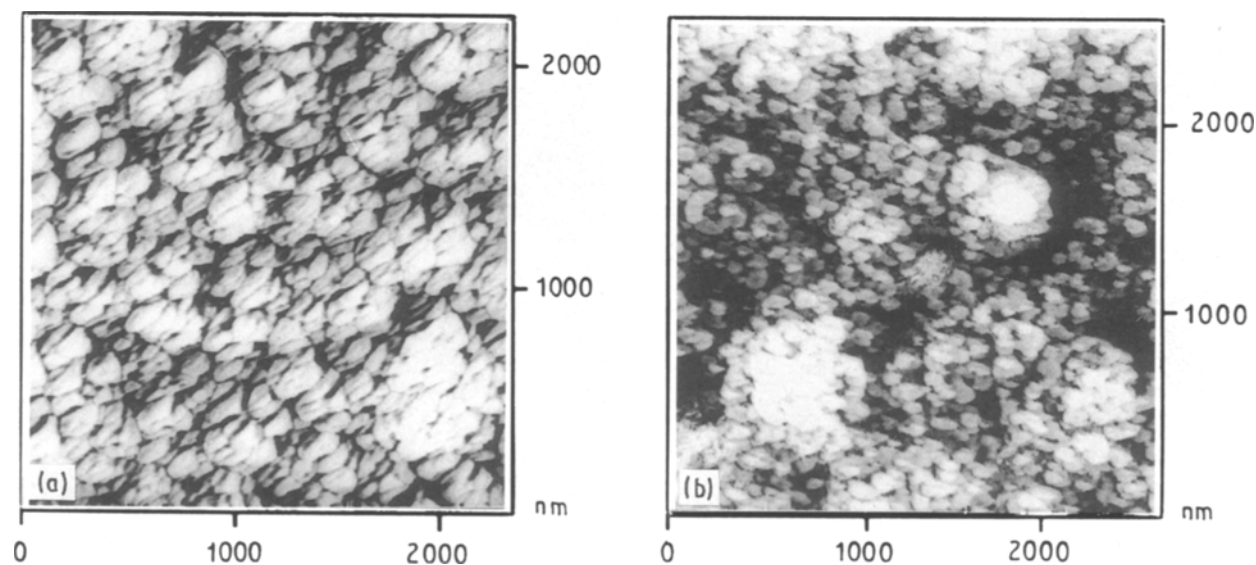


Figure 4 STM image of the surface morphology of thin films deposited on  $\text{LaAlO}_3$  at the different deposition rates of (a) 1 and (b) 50 Hz; maximum height in the  $z$ -direction is 20 nm.

Recent work from this laboratory as well as other laboratories has been directed at producing highly textured films on polycrystalline substrates. Interestingly thin films of  $\text{YBa}_2\text{Cu}_3\text{O}_{7-x}$  on both polycrystalline zirconia [13] and silver foil [15] are highly textured with surprisingly high  $J_c$  values (in the range  $10^5$ – $10^6$   $\text{A cm}^{-2}$ ). The texturing is perhaps not too surprising because the texturing reflects the anisotropic growth kinetics of the Y-123 films, with the most rapid growth in the  $a$ - $b$  plane. It is not clear why such high  $J_c$  values are found because there is no obvious mechanism for producing the required low-angle grain boundaries. Therefore we looked at the morphology of *in situ* laser-deposited films on silver foil. Details of this work can be found in [16]. The STM images of these surfaces (Fig. 5) were radically different from all of the other substrates studied. In particular, very large chip-like structures (presumably large crystallites) with a high amount of texture were imaged. The surface crystallite size is typically 300 nm, as compared to about 10 nm on MgO. The exact reason for the increased grain size is not clear, although it has been noted in the past that silver can act as a flux to enhance grain growth.

In the course of this work, we also discovered that chemical etching is a very useful technique for probing the sub-structure of the high  $T_c$  thin films grown on various substrates. Such information allows one to build a clearer picture of the entire film structure from which a growth model can be proposed with the assumption that the etching proceeds in a fashion opposite to that of growth.

It is well known in the literature that bromine in methanol is a very effective etch for the surface of the high-temperature superconductors [11]. We have chemically etched a 100 nm thick film of  $\text{YBa}_2\text{Cu}_3\text{O}_{7-x}$  deposited on  $\text{LaAlO}_3$  for times of up to 5 min in this etchant. At longer etch times, imaging the surface requires the use of AFM because the material becomes non-conductive. A series of images

of chemically etched surfaces can be found in Fig. 6. The most striking feature is that the individual grains become evident as the film is etched. In between many of the grains the material is completely removed down to the extremely flat substrate. This etching effect reflects the granular nature of these films and suggests these films are better described as aligned polycrystalline films rather than simply single crystal type films. The structures that are observed, the formation of the individual grains, suggests that  $\text{Br}_2/\text{MeOH}$  is a preferential etchant attacking the grain boundaries and etching the grains back to low-index faces parallel to the  $c$ -axis which represent the densest areas of the films which have grown up. The size of the grains is 75–300 nm, consistent with a number of TEM studies of grain sizes within thin films of this type [2, 17]. As the etching continues, the grains become reduced in size and number. The etched structures that are observed probably represent individual and yet completely aligned grains (due to the epitaxial growth nature of these films with high orientation). The ability to form such structures may have implications for device applications. The precise shape of the grains may reflect the mutual alignment between the grains; however, it is also possible that the exact shape observed is related to the pyramidal shape of the micro-machined tip. Further work is in progress to address this. Perhaps the main point to note, however, is that the films are chemically etched to individual islands which may support the formation of islands in the growth of such films. It appears that chemical etching coupled with force microscopy appears to be a very useful technique for examining the internal micro-structure of the deposited thin films.

Assuming that each grain nucleates on a defect on the substrate then the chemical etching method may prove of particular value to estimate the number of nucleation sites within a film. Such factors may be of particular importance with respect to flux-pinning effects [8, 9]. A nice feature of the present technique of

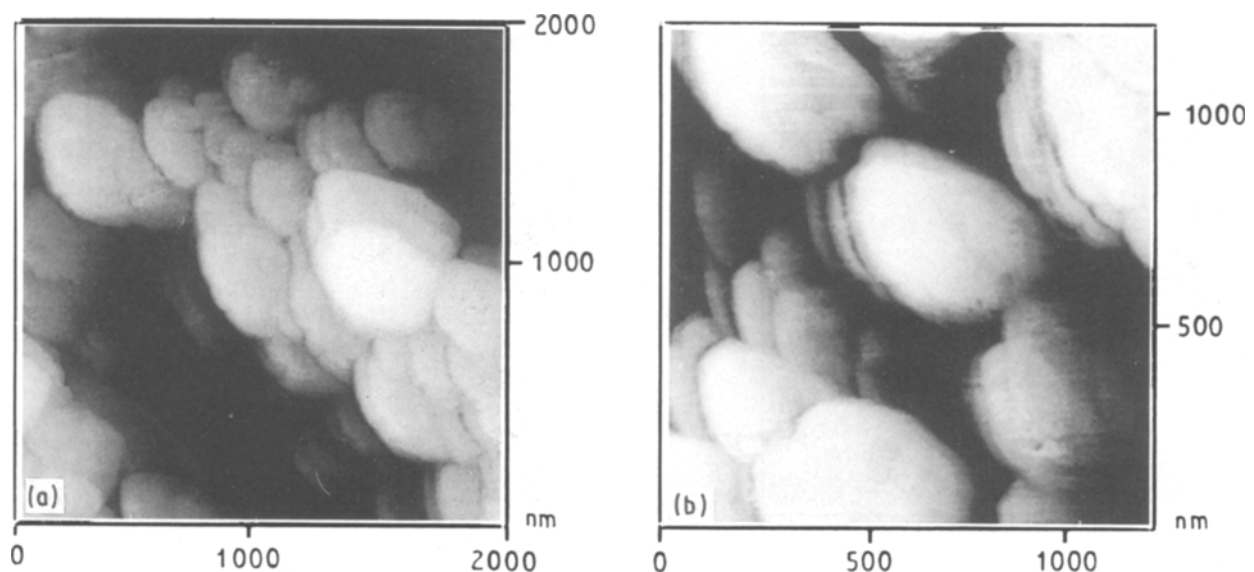


Figure 5 STM image of the surface morphology of thin films deposited on polycrystalline silver foil at different magnifications, showing the increase in crystallite size.

chemical etching and viewing is that high detail of the substructure is observed.

The data presented on both the surface morphologies (chips or islands) and chemically etched struc-

tures (aligned and oriented grains) appears consistent with the Stranski-Krastanov model for nucleation and growth of thin films [18]. As pulses of material reach the surface, nucleation occurs at a number of

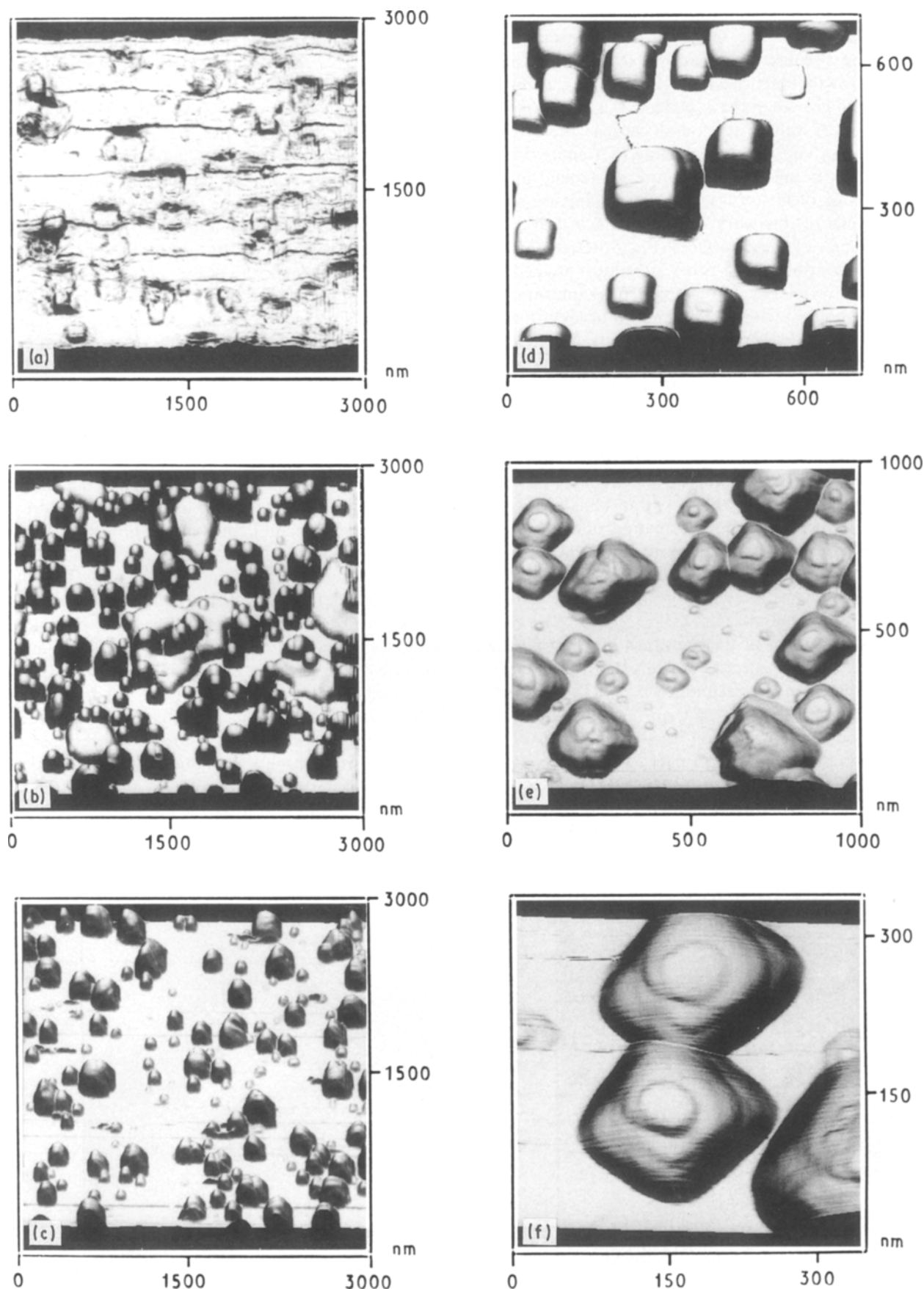


Figure 6 AFM images of a 100 nm film which has been chemically etched for varying times with 0.5% bromine-in-methanol. Chemical etch times are (a) 15 s, (b) 1, (c) 2 and (d-f) 5 min. (b-d) show the high degree of grain alignment. (d, f) Tilted at 45° to clearly show the morphology with chips in the centre. The highest grains are about 100 nm.



sites on the surface. Possible nucleation sites may be steps or other defects present on the surface of the substrate. The distinct grains which are evident upon chemical etching may represent initial nucleation sites. Minimizing the thin film surface energy results in grains with the preferred *c*-axis orientation normal to the surface, with the best fit of the two oxygen sublattices at the substrate/film interface. On continued deposition, these islands grow in size and number to form aligned grains (as observed in the chemical etching studies). As the area of the islands increases, they offer the opportunity for nucleation of new islands on the growing layer leading to the terraced structure observed. These grains will then grow and eventually coalesce into a fully aligned and oriented thin film. The surface morphology may, therefore, reflect the overall growth pattern throughout the entire film.

It is also of interest to compare our data with the recent studies on sputtered films [8, 9]. Although we do not see distinct spiral growth features, we do see structures consistent with the spiral growth under what may be different kinetic conditions. Also the appearance of terraces is similar. In the etching studies the sub-structure of the film is consistent with a spiral growth effect. It appears that the growth mechanism may be similar between these different techniques. Subtle differences in surface morphologies are apparent. It is likely that in some areas of the film, the grains or columns grow via screw dislocations, that is by adding atoms to a spirally expanding step on the top surface of the grain. This would, in fact, explain the columnar structures observed. The fact that differences are observed is perhaps not too surprising, because sputtering is a continuous process, whereas laser ablation deposits material in pulses where more supersaturation is likely. Further work will be required to elucidate and fully understand the differences between films grown via the different techniques.

In summary, we have found that STM is a very useful tool for studying the surface morphology of thin films of high-temperature superconductors. In particular, the surface appears as pinnacles or stacks which contain chip-like morphologies or terraces at the surface. The substructure is much more continuous. When these films are chemically etched, very striking sub-structures are revealed using AFM which show individual grains, mutually aligned but distinct on the substrate. The data are consistent with a thin-film growth pattern based on nucleation and growth

with a screw dislocation being a possible source of the terraced structures.

## Acknowledgements

We thank Sue Riggs and Ed Delawski for technical assistance.

## References

1. M. G. NORTON and C. B. CARTER, *Phys. C* **172** (1990) 47.
2. R. RAMESH, T. S. RAVI, D. M. HWANG, C. C. CHANG, A. INAM, T. VENKATESAN, X. D. WU, R. E. MUENCHAUSEN, S. FOLTYN and N. S. NOGAR, *ibid.* **173** (1991) 163.
3. D. H. SHIN, J. SILCOX, S. E. RUSSEK, D. K. LATHROP, B. MOECKLY and R. A. BUHRMAN, *Appl. Phys. Lett.* **57** (1990) 508.
4. D. M. HWANG, T. VENKATESAN, C. C. CHANG, L. NAZAR, X. D. WU, A. INAM and M. S. HEGDE, *ibid.* **54** (1989) 1702.
5. C. B. EOM, A. F. MARSHALL, S. S. LADERMAN, R. D. JACOWITZ and T. H. GEBALLE, *Science* **249** (1990) 1549.
6. C. C. CHANG, X. D. WU, R. RAMESH, X. X. XI, T. S. RAVI, T. VENKATESAN, D. M. HWANG, R. E. MUENCHAUSEN, S. FOLTYN and N. S. NOGAR, *Appl. Phys. Lett.* **57** (1990) 1814.
7. N. G. CHEW, S. W. GOODYEAR, J. A. EDWARDS, J. S. SATCHELL, S. E. BLENKINSOP and R. G. HUMPHREYS, *ibid.* **57** (1990) 2016.
8. C. GERBER, D. ANSELMETTI, J. G. BEDNORZ, J. MANNHART and D. G. SCHLOM, *Nature* **350** (1991) 279.
9. M. HAWLEY, I. D. RAISTRICK, J. G. BEERY and R. J. HOULTON, *Science* **251** (1991) 1587.
10. B. PARKINSON, *J. Amer. Chem. Soc.* **112** (1990) 7498.
11. M. GURVITCH, J. M. VALLES Jr, A. M. CUCOLO, R. C. DYNES, J. P. GARNO, L. F. SCHNEEMEYER and J. V. WASZCZAK, *Phys. Rev. Lett.* **63** (1989) 1008.
12. P. K. HANSMA, V. B. ELINGS, O. MARTI and C. E. BRACKER, *Science* **242** (1988) 209.
13. D. P. NORTON, D. H. LOWNDES, J. D. BUDAI, D. K. CHRISTEN, E. C. JONES, K. W. LAY and J. E. TKACZYK, *Appl. Phys. Lett.* **57** (1990) 1164.
14. M. A. HARMER, C. R. FINCHER and B. A. PARKINSON, *J. Appl. Phys.*, **70** (1991) 2760.
15. J. ZHAO, Y. Q. LI, C. S. CHERN, P. NORRIS, B. GALLOIS, B. KEAR and B. W. WESSELS, *Appl. Phys. Lett.* **58** (1991) 89.
16. G. B. BLANCHET, C. R. FINCHER and S. I. SHAH, *Supercond. Sci. Tech.*, in press.
17. C. VIGNOLLE and A. GERVAIS, *Mater. Res. Bull.* **26** (1991) 171.
18. K. REICHELTL, *Vacuum* **18** (1988) 1083.

Received 1 May

and accepted 9 September 1991